

Internal consistency in the close-coupling approach to positron collisions with atoms^{*}

Igor Bray^a, Jackson J. Bailey, Dmitry V. Fursa, Alisher S. Kadyrov, and Ravshanbeck Utamuratov

Curtin Institute of Computation and Department of Physics, Astronomy and Medical Radiation Sciences, Curtin University, GPO Box U1987, Perth, WA 6845, Australia

Received 20 October 2015 / Received in final form 24 November 2015

Published online 12 January 2016 – © EDP Sciences, Società Italiana di Fisica, Springer-Verlag 2016

Abstract. The positron-atom scattering problem contains the rearrangement channel of positronium (Ps) formation. While this makes the problem particularly difficult to calculate, it has the unusual benefit of validation via consideration of the internal consistency of the vastly different one- and two-centre close-coupling approaches. For example, the ionisation cross section in the former must be the same as the sum of breakup and Ps formation cross sections in the latter. This places a severe test on both approaches, which we review here for positron scattering on hydrogen and helium atoms.

1 Introduction

During the last two decades there has been considerable progress in calculation of electron scattering on atoms. For the simplest targets such as H and He, elastic scattering, excitation and ionisation can be routinely calculated at all energies of interest [1–4]. The application to differential ionisation cross sections allowed the resolution of the long-standing formal problems associated with breakup collisions involving the long-ranged Coulomb potentials [5,6] and explained the success of the numerical methods [7].

The corresponding positron scattering problems are more complicated due to the existence of the positronium (Ps) formation reaction channel, requiring a two-centre approach to the problem. The two centres, atom and Ps, have their own discrete spectrum and their own continuum. While at large separation the two sets of corresponding discrete wavefunctions do not overlap, the two continua do. This makes an approach to the solution based on the expansion with states of the two centres inherently problematic. Yet positron scattering is not only of interest in its own right, but also is a prototype of the ubiquitous proton scattering problems, where formation of atomic hydrogen is an important reaction channel. Consequently, a systematic approach to problems containing rearrangement channels such as Ps or H-formation is required.

Despite the issue of overlapping continua the two-centre convergent close-coupling (CCC) approach has been very successful in obtaining convergent results

for e^+ -H scattering [8–10]. It is based on the momentum-space approach of Mitroy [11–13]. Similar approaches in coordinate space were undertaken by Kernoghan et al. [14,15]. The major aspect that distinguishes the CCC approach from others is the capacity to take sufficiently large basis sizes which enable demonstration of convergence. The usage of the complete Laguerre basis ensures that completeness is approached by simply taking more basis functions.

By convergence we generally mean systematically increasing the size of the CCC calculations until variation of the results is within the desired accuracy. However, here we wish to examine a different kind of convergence: this is the mutual convergence of the rather disparate one- and two-centre CCC approaches to the positron-atom scattering problem. When these two approaches independently converge to the same result we refer to this as demonstrating internal consistency of the CCC method. This is a form of validation of both approaches, without reference to experiment, something that is not available in electron-atom scattering calculations. A preliminary discussion of these ideas has already been undertaken for the zeroth partial wave of positron-hydrogen scattering [16].

2 One- and two-centre approaches to positron-atom scattering calculations

The close-coupling approach to electron or positron scattering on atoms is based on expanding the total wavefunction of the scattering system using a complete set of eigenstates of the target Hamiltonian H_T . In the case of atomic hydrogen these would be the countably infinite discrete states and the uncountably infinite continuum states. Since numerically it is too difficult to implement

^{*} Contribution to the Topical Issue “Advances in Positron and Electron Scattering”, edited by Paulo Limao-Vieira, Gustavo Garcia, E. Krishnakumar, James Sullivan, Hajime Tanuma and Zoran Petrovic.

^a e-mail: I.Bray@curtin.edu.au

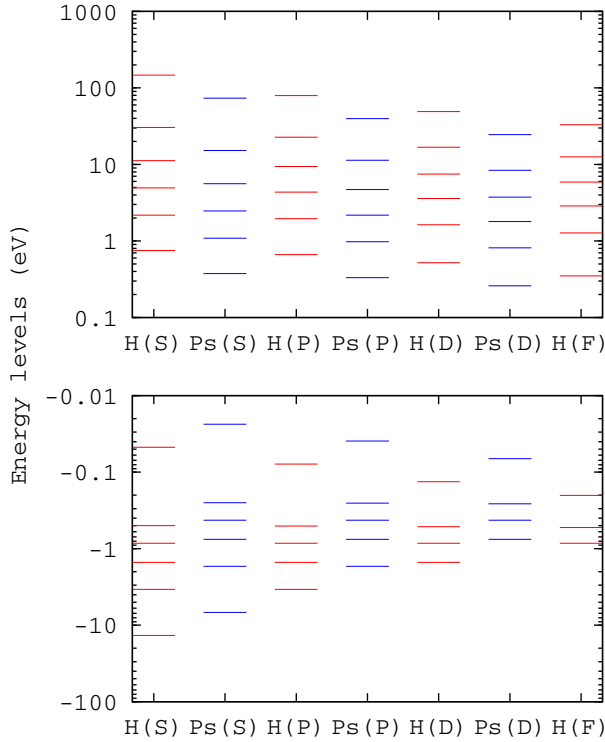


Fig. 1. Energies in the CCC(123,122) positron-hydrogen calculations. Here $12 - l$ states were obtained for each l via equation (2) with $\lambda_l^H = 1$ and $\lambda_l^{Ps} = 0.5$.

the target continuum states directly, we rely on square-integrable (L^2) expansions instead. The CCC method [1] utilises the complete Laguerre basis for an orbital angular momentum l

$$\xi_{kl}(r) = \sqrt{\frac{\lambda_l(k-1)!}{(2l+1+k)!}} (\lambda_l r)^{l+1} \exp(-\lambda_l r/2) L_{k-1}^{2l+2}(\lambda_l r), \quad (1)$$

where the $L_{k-1}^{2l+2}(\lambda_l r)$ are the associated Laguerre polynomials, and k ranges from 1 to the basis size N_l . The constant λ_l is arbitrary and is chosen so that the lowest energy states are essentially the exact eigenstates. The orthonormal target states ϕ_n are made of linear combinations of the Laguerre functions and satisfy

$$\langle \phi_f | H_T | \phi_i \rangle = \varepsilon_f \delta_{fi}. \quad (2)$$

To reduce the number of parameters when making systematic studies of convergence we typically set $\lambda_l = \lambda$, and $N_l = N_0 - l$ for $0 \leq l \leq l_{\max}$. Then we have just two parameters N_0 and l_{\max} to vary. We succinctly label such calculations by $N_{l_{\max}}$, where $N = N_0$.

In the case of positron-atom scattering there are two target Hamiltonians. In addition to the atomic Hamiltonian there is also the Ps Hamiltonian, which yields Ps states by solving equation (2) as well. A typical example of the energies ε_f arising in positron-hydrogen calculations are given in Figure 1. Here the lower negative-energy states are the true eigenstates of the H and Ps

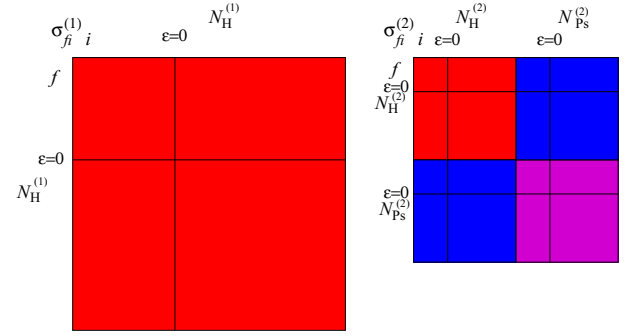


Fig. 2. Matrix overview of the cross sections σ_{fi} arising from one-centre (left) and two-centre (right) CCC positron-hydrogen calculations. Explicit Ps-formation cross sections arise only in two-centre calculations, but the effect of Ps formation in one-centre calculations is taken into account by the positive-energy atomic states, see text.

Hamiltonians. The positive-energy states correspond to the three-body breakup process, and both the H and Ps states contribute to this from their separate centres. This would seem problematic when two complete bases are used to describe the same collision process.

The details of the two-centre CCC theory for positron scattering on atomic hydrogen and helium have been given by Kadyrov and Bray [9] and Utamuratov et al. [17,18], respectively. Rather than reproducing the mathematical detail, we explain the difference between the one- and two-centre CCC approaches with the aid of Figure 2.

In the one-centre CCC method the resulting cross sections $\sigma_{fi}^{(1)}$ involve only direct atom-atom transitions between all included initial i and final f atomic states. These calculations are a simplification of electron scattering by elimination of exchange, and change of sign on the potentials. However, convergence in these calculations is particularly slow with increasing $l_{\max}^{(1)}$. The large- l states effectively take into account Ps formation and breakup processes. For this reason we have drawn the one-centre calculation matrix in Figure 2 considerably larger than the two-centre calculation matrix. In practice the speed of calculating the interaction elements in the simple one-centre case is so much faster that the increased matrix size is of little consequence. At positron energies above the ionisation threshold (13.6 eV) there is no way to distinguish between Ps formation and breakup processes, but the electron-loss cross section (sum of Ps formation plus breakup) should be convergent. In the extended Ore gap, between 6.8 eV and 13.6 eV, there is no way to represent real Ps formation. We shall see that whenever Ps formation is not negligible this manifests itself as a lack of convergence. At positron energies below the Ps formation threshold (6.8 eV) convergence to the correct elastic scattering cross section is expected, though large $l_{\max}^{(1)}$ are required due to the importance of virtual Ps formation.

The two-centre calculations, yielding cross sections $\sigma_{fi}^{(2)}$, are more complicated due to the existence of the atom-Ps rearrangement channels. The atom-atom

component is the same as in the one-centre case though much smaller $l_{\max}^{(2)}$ are required for convergence. While we have drawn the (blue) atom-Ps matrix to be similar in size as the (red) atom-atom matrix, the former interaction elements take at least an order of magnitude longer to calculate. However, now all physical processes are explicitly included and should be convergent at all energies. Inclusion of explicit Ps formation channels ensures that their virtual and real contributions are taken into account with relatively small basis sizes, such as those presented in Figure 1. In fact the primary driver of the requirement for larger bases is the breakup channel. As in electron scattering, this is associated with the positive-energy states and requires a sufficiently large discretisation to yield convergent results close to the breakup threshold.

2.1 Internal consistency of the one- and two-centre close coupling methods

We are now in a position to discuss what we mean by validation of the two approaches via internal consistency checks. Due to the completeness of the Laguerre basis, even the one-centre CCC calculations can yield correct results. Specifically, at energies outside the extended Ore gap, for discrete ($\varepsilon_f^A, \varepsilon_i^A < 0$) atomic transitions we must have the two approaches independently converge such that

$$\sigma_{fi}^{(2)} = \sigma_{fi}^{(1)}. \quad (3)$$

Furthermore, at energies above the breakup threshold

$$\sigma_{\text{eloss}}^{(2)} = \sigma_{\text{Ps}}^{(2)} + \sigma_{\text{brk}}^{(2)} = \sigma_{\text{ion}}^{(1)}, \quad (4)$$

where for some initial state i

$$\sigma_{\text{Ps}}^{(2)} = \sum_{f: \varepsilon_f^{\text{Ps}} < 0} \sigma_{fi}^{(2)}, \quad (5)$$

$$\sigma_{\text{brk}}^{(2)} = \sum_{f: \varepsilon_f^{\text{Ps}} > 0} \sigma_{fi}^{(2)} + \sum_{f: \varepsilon_f^A > 0} \sigma_{fi}^{(2)}, \quad (6)$$

$$\sigma_{\text{ion}}^{(1)} = \sum_{f: \varepsilon_f^A > 0} \sigma_{fi}^{(1)}. \quad (7)$$

Note that in the case of one-centre calculations there is no explicit Ps formation, and so ionization is synonymous with breakup. In the two-centre case we are careful to distinguish between Ps-formation and breakup (ionisation with no Ps formation) processes, and so we avoid the word ionisation.

To demonstrate internal consistency succinctly it is useful to look at the total cross sections (TCS), which by equations (3) and (4) must satisfy

$$\begin{aligned} \sigma_{\text{TCS}}^{(2)} &= \sum_{\varepsilon_f^A}^{N_A^{(2)}} \sigma_{fi}^{(2)} + \sum_{\varepsilon_f^{\text{Ps}}}^{N_{\text{Ps}}^{(2)}} \sigma_{fi}^{(2)}, \\ &= \sigma_{\text{TCS}}^{(1)} = \sum_{f=1}^{N_A^{(1)}} \sigma_{fi}^{(1)}. \end{aligned} \quad (8)$$

At energies below the Ps-formation threshold the TCS is just elastic scattering, and so both approaches should agree. At energies above the breakup threshold the TCS is the sum of discrete excitation and electron-loss cross sections, and so again both approaches should agree. However, in the extended Ore gap only the two-centre calculations can yield convergent results.

2.2 Positron-hydrogen scattering

We begin our check of internal consistency by considering in Figure 3 positron-hydrogen scattering cross sections over a broad energy range, for partial waves of total orbital angular momenta $L \leq 5$, as well as summed over all L . For the one-centre calculation we took $30 - l$ Laguerre-based states for $l_{\max}^{(1)} = 9$. These are labeled CCC(30g, 0), and a total of 255 states with a maximum of 1320 coupled channels. The two-centre calculations presented here are of the symmetric type where $20 - l$ states are taken for both the H and Ps centres, with $l_{\max}^{(2)} = 2$ also being the same for both centres. These calculations are labeled CCC(20₂, 20₂), and have 114 states and a maximum of 224 coupled channels. In addition to the TCS, the electron-loss cross sections are also presented to directly check equation (4). Total Ps-formation cross sections for the discrete and continuum states are also given on the left and right sides of the figure, respectively.

Starting with the zeroth partial wave, we see good agreement for the TCS at all energies. This is as expected, except perhaps in the extended Ore gap. The reason the two calculations agree even here is that the Ps-formation cross section (visible in the electron-loss panel) is particularly small for this partial wave. We shall see that this is not the case for higher partial waves. Turning our attention to the electron-loss cross sections, we see excellent agreement between the two calculations except in the region just above the breakup threshold. This region is dominated by Ps formation, which can only be reproduced by low positive-energy atomic pseudostates. In other words, the one-centre calculations should yield a step-function: zero below the breakup threshold, and the Ps formation cross section immediately above. From Figure 1 it is clear that very large basis sizes would be required to ensure a fine energy-discretisation, and so it will never be practical to yield an actual step-function. Nevertheless, a rapid rise is expected past the breakup threshold, and since the breakup cross section starts from zero, the one-centre calculation does give a good estimate of Ps-formation just above the breakup threshold as soon as convergence is reached. Lastly, the Ps formation in the continuum component (second part of Eq. (6)) is clearly visible, and so contributes substantially to ensuring that equation (4) is satisfied. Even though both parts of the R.H.S. of Eq. (6) represent a breakup process, unitarity of the close-coupling method ensures no double-counting.

For partial wave $L = 1$ we again see the expected good agreement between the two calculations of the TCS outside the extended Ore gap. This time Ps formation

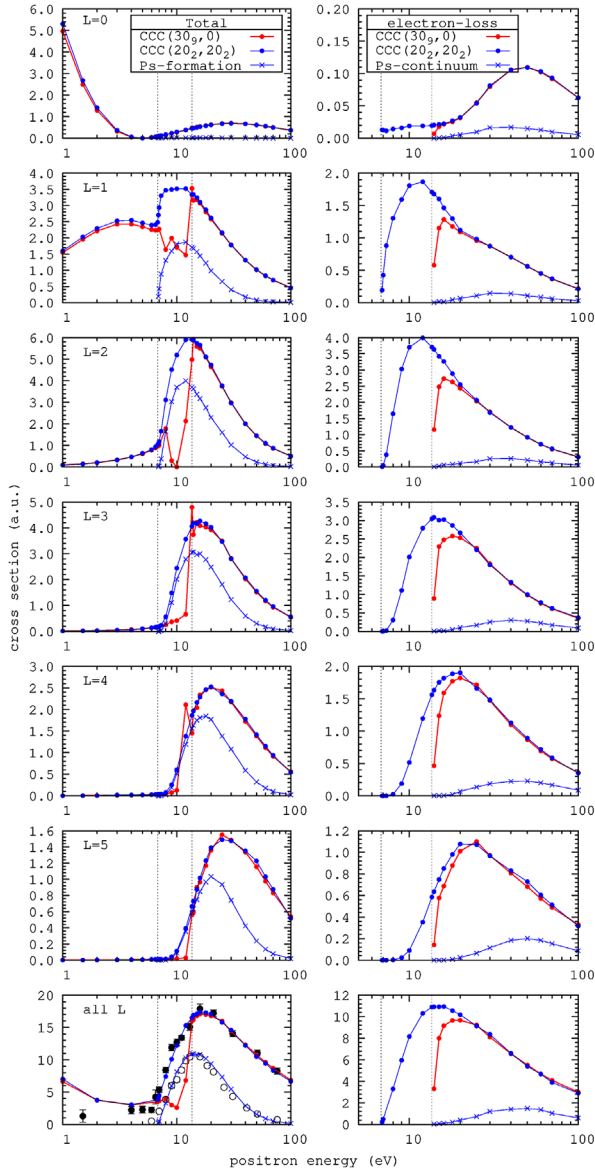


Fig. 3. Total and electron-loss (Ps formation plus breakup) cross sections for positron scattering on atomic hydrogen for specified partial waves L obtained using the one- two-centre CCC calculations, see text. The indicated points corresponding to the energies at which the calculations were performed are connected with straight lines to guide the eye. The vertical lines are the Ps formation and breakup thresholds, spanning the extended Ore gap. The experimental data in the bottom left panel are due to Zhou et al. [19].

in the Ore gap is substantial which is cannot be treated in any way by the one-centre CCC($30_9, 0$) calculations. Moving across to the electron-loss cross sections we see the expected good agreement between the calculations at energies above the breakup threshold. Now that the Ps-formation cross section is clearly visible (on the TCS panel) the one-centre calculations yield similar values for electron-loss cross sections in the region soon after the breakup threshold.

The behaviour for partial waves $2 \leq L \leq 5$ is much the same as for $L = 1$, with the quantitative trends now of particular interest. The Ps-formation cross section maximum occurs for $L = 2$, and even the $L = 5$ component is considerably larger than for $L = 0$. It is also interesting to see how the Ps-formation cross section peak moves to higher energies with increasing L . This contributes to the peak of the electron-loss cross section also moving to higher energies with increasing L . Additionally, the reproduction of the Ps-formation cross section by CCC($30_9, 0$) near the breakup threshold becomes easier with increasing L .

Having validated the two approaches against each other internally for individual partial waves, we are now in a position to sum them all, and add higher partial waves, in order to compare with experiment. This is done in the bottom left panel of Figure 3, where we compare the CCC results with the TCS and Ps formation measurements of Zhou et al. [19]. We see excellent agreement with experiment with the exception of low energies. It is not our aim here to provide a comprehensive comparison with other theory and experiment, which has been done earlier [9], but instead to emphasize that the demonstrated internal consistency indicates that we can remain confident in the results of the CCC calculations even when discrepancy with experiment is found.

2.3 Positron-helium scattering

We next turn our attention to the helium target. Whereas the one-centre approach to positron scattering is a trivial application of the e-He CCC theory [2] (dropping exchange and changing the sign on the potentials), the two centre CCC approach is much more complicated [17,18]. Unlike in the positron-hydrogen system, where Ps formation leads to a residual bare proton, for helium the residual ion is He^+ , which may even be in an excited state (including the continuum). Furthermore, the symmetry conditions of the two electrons in helium should be preserved throughout the collision, which is problematic once Ps formation takes place. In addition to the above conceptual problems, we now have to deal with two-electron states, which are treated to a finite level of numerical precision, whereas for hydrogen the one-electron states availed themselves of analytical techniques. This is particularly problematic when ill-conditioned systems require high precision. These issues affect only the two-centre CCC approach, but not the one-centre one. Accordingly, validation via internal consistency takes on a considerably more complex prospect for multielectron targets, of which helium is the most fundamental example.

Though the details of positron scattering on helium are rather more complicated than for atomic hydrogen, the internal consistency ideas already discussed are equally applicable. In particular, Figure 1 would be much the same, except for hydrogen state energies replaced by singlet helium state energies. Figure 2 is equally applicable with N_{H} replaced by N_{He} . Convergence concepts are also the same, as are the labels for the CCC calculations.

In Figure 4 we present a detailed study of internal consistency of the one- and two-centre CCC calculations for positron-helium scattering. The CCC(30₉, 0) are convergent one-centre calculations, but only in the region outside the extended Ore gap. The CCC(20₂, 20₂) are analogous to those for the atomic hydrogen target, except that in both cases we now have to be more careful in how the two-electron states are obtained utilising Laguerre functions. Specifically, we use a multiconfiguration description of the helium 1S symmetry with “frozen-core” $\{1s, nl\}$ configurations for all other 1L symmetries. To improve on the frozen-core approach for the 1S states we add short-ranged $\{nl, n'l'\}$ for $n, n' \leq 3$ and $l, l' \leq 2$. The resulting ground state ionisation energy is 24.5 eV (an error of 0.1 eV), which is of considerable improvement on the frozen-core energy of 23.8 eV. For $N_0 = 30$ and $l_{\max} = 9$ we end up with 37 1S states, and $30 - l$ singlet states with $1 \leq L = l \leq 9$. Such calculations have a total of 262 states with a maximum of 1327 coupled channels. With $N_0 = 20$ and $l_{\max} = 2$ we end up with 27 1S states, 19 1P states and 18 1D states. The Ps states are the same as in the hydrogen target case, resulting in a calculation with 121 states and a maximum of 231 coupled channels (seven more of both than for hydrogen).

In Figure 4 we repeat the check of internal consistency, but this time for the helium target. The two-centre results are very sensitive to the internal numerics due to the inherently ill-conditioned two-centre approach. Consequently, the two-centre results presented show some minor unphysical oscillations, but cannot be readily improved. Comparison with the one-centre results gives an indication of the associated uncertainties. In the one-centre calculations there is full antisymmetry and the multiconfiguration treatment allows for ionisation plus excitation processes. They correspond to breakup plus excitation and Ps-formation plus excitation. Consequently, we expect the one-centre results to be the more accurate (outside the Ore gap).

Beginning with the zeroth partial wave, we see good agreement of the two calculations for the TCS, and somewhat less so for the electron-loss cross section. Just like in the case of H, for He the Ps-formation cross section for this partial wave is very small and so the TCS is in good agreement even in the extended Ore gap.

The next partial wave has a substantial Ps-formation cross section in the extended Ore gap, and consequently the one-centre results fail to yield accurate results there. Outside this gap the agreement between the two calculations shows a minor discrepancy, with the two-state results being generally above the one-centre ones. The same is true for the next partial wave ($L = 2$). However, with increasing partial waves the two calculations come together, with agreement similar to that found for atomic hydrogen.

Summing the results for all of the presented partial waves, and adding higher ones to convergence, we are able to compare with experiment. This time, unlike in the case of H, we have good agreement with experiment down to very low energies. The small differences between the two calculations for the lower partial waves become negligible

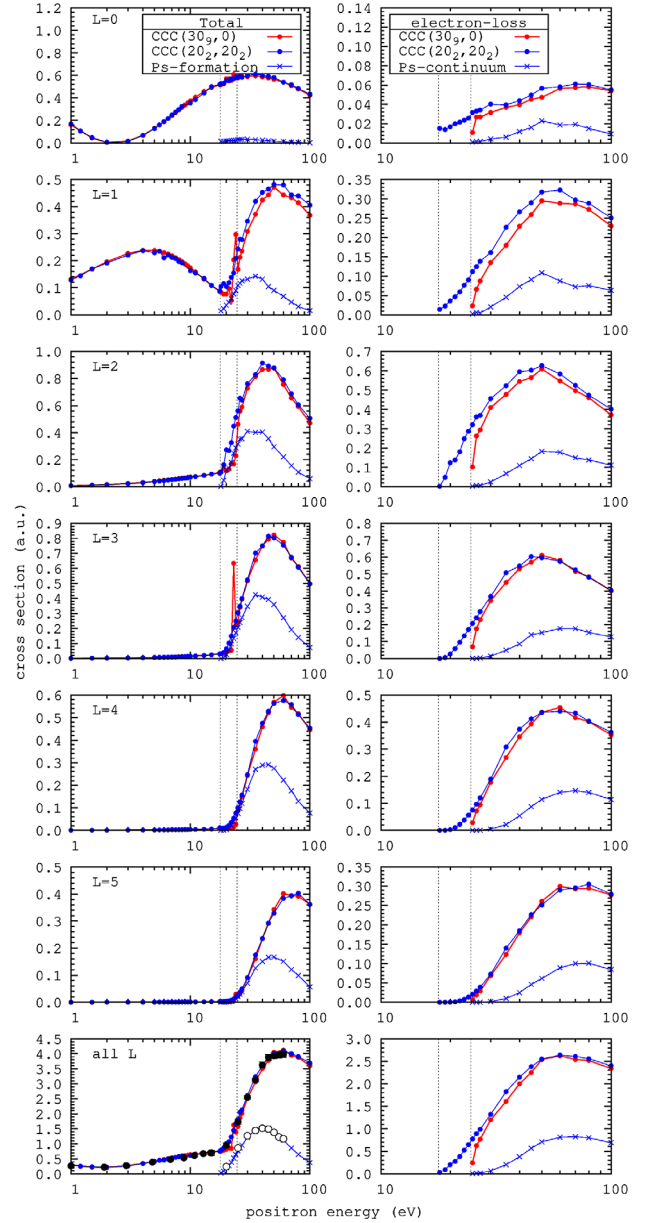


Fig. 4. Same as for Figure 3 except of positron-helium scattering. The experimental data in the bottom left panel are due to Sullivan et al. [20] and Caradonna et al. [21].

when summed over all partial waves. Nevertheless, there is some work to be done to improve the agreement for the lower ones.

3 Conclusions

We presented the most detailed to date study of internal consistency checks of positron scattering on atomic hydrogen and helium. This check is unique to problems that can be tackled using both one- and two-centre approaches, and can be performed for individual partial waves. In the case of hydrogen the agreement between the two approaches is as expected: excellent outside the extended Ore gap.

For helium the agreement is still satisfactory, though some minor discrepancies are evident. These internal consistency checks are very helpful in determining the accuracy, and hence the uncertainty, of the calculations.

Such tests can also be performed for two-centre implementations of positron scattering from alkali targets [22,23], alkaline earth metals [24] and the hydrogen molecule [25]. We expect that these targets will form an even more formidable challenge.

The same ideas are equally applicable to proton (ion) scattering on atoms and molecules. In such cases the projectile acts as the second centre allowing for an explicit treatment of the electron-transfer process. The first test, of proton scattering on atomic hydrogen, is particularly promising [26].

Author contribution statement

All authors contributed equally to the paper.

We would like to thank the organisers of the POSMOL 2015 Workshop for the invitation to present the above work. We also take the opportunity to congratulate Prof. Michael Allan upon his retirement, and thank him for the many fruitful interactions. The support of the Australian Research Council, the Australian National Computer Infrastructure and the Pawsey Supercomputer Centre are gratefully acknowledged.

References

1. I. Bray, A.T. Stelbovics, Phys. Rev. A **46**, 6995 (1992)
2. D.V. Fursa, I. Bray, Phys. Rev. A **52**, 1279 (1995)
3. I. Bray, Phys. Rev. Lett. **89**, 273201 (2002)
4. A.T. Stelbovics, I. Bray, D.V. Fursa, K. Bartschat, Phys. Rev. A **71**, 052716(13) (2005)
5. A.S. Kadyrov, I. Bray, A.M. Mukhamedzhanov, A.T. Stelbovics, Phys. Rev. Lett. **101**, 230405 (2008)
6. A.S. Kadyrov, I. Bray, A.M. Mukhamedzhanov, A.T. Stelbovics, Ann. Phys. **324**, 1516 (2009)
7. I. Bray, D.V. Fursa, A.S. Kadyrov, A.T. Stelbovics, A.S. Kheifets, A.M. Mukhamedzhanov, Phys. Rep. **520**, 135 (2012)
8. A.S. Kadyrov, I. Bray, J. Phys. B **33**, L635 (2000)
9. A.S. Kadyrov, I. Bray, Phys. Rev. A **66**, 012710 (2002)
10. A.S. Kadyrov, I. Bray, A.T. Stelbovics, Phys. Rev. Lett. **98**, 263202 (2007)
11. J. Mitroy, Aust. J. Phys. **48**, 893 (1995)
12. J. Mitroy, Aust. J. Phys. **48**, 645 (1995)
13. J. Mitroy, J. Phys. B **29**, L263 (1996)
14. A.A. Kernoghan, M.T. McAlinden, H.R.J. Walters, J. Phys. B **28**, 1079 (1995)
15. A.A. Kernoghan, D.J.R. Robinson, M.T. McAlinden, H.R.J. Walters, J. Phys. B **29**, 2089 (1996)
16. J.J. Bailey, A.S. Kadyrov, I. Bray, Phys. Rev. A **91**, 012712 (2015)
17. R. Utamuratov, A.S. Kadyrov, D.V. Fursa, I. Bray, A.T. Stelbovics, J. Phys. B **43**, 125203 (2010)
18. R. Utamuratov, A.S. Kadyrov, D.V. Fursa, I. Bray, J. Phys. B **43**, 031001 (2010)
19. S. Zhou, H. Li, W.E. Kauppila, C.K. Kwan, T.S. Stein, Phys. Rev. A **55**, 361 (1997)
20. J.P. Sullivan, C. Makochekeanwa, A. Jones, P. Caradonna, S.J. Buckman, J. Phys. B **41**, 081001 (2008)
21. P. Caradonna, A. Jones, C. Makochekeanwa, D.S. Slaughter, J.P. Sullivan, S.J. Buckman, I. Bray, D.V. Fursa, Phys. Rev. A **80**, 032710 (2009)
22. A.V. Lugovskoy, A.S. Kadyrov, I. Bray, A.T. Stelbovics, Phys. Rev. A **82**, 062708 (2010)
23. A.V. Lugovskoy, A.S. Kadyrov, I. Bray, A.T. Stelbovics, Phys. Rev. A **85**, 034701 (2012)
24. R. Utamuratov, D.V. Fursa, A.S. Kadyrov, A.V. Lugovskoy, J.S. Savage, I. Bray, Phys. Rev. A **86**, 062702 (2012)
25. R. Utamuratov, A.S. Kadyrov, D.V. Fursa, M.C. Zammit, I. Bray, Phys. Rev. A **92**, 032707 (2015)
26. I.B. Abdurakhmanov, A.S. Kadyrov, I. Bray, J. Phys. B accepted (2015)